Analysis of particle p_T-spectra in model-generated HICs using Tsallis statistics

E. Zabrodin,
in collaboration with
P. Panasiuk and L. Bravina

XII-th International Conference on New Frontiers in Physics ICNFP-2023
Kolymbari, Crete, Greece, 10 -- 23.07.2023

Motivation

Search for equilibrium

Relativistic heavy-ion collisions: Thermal model

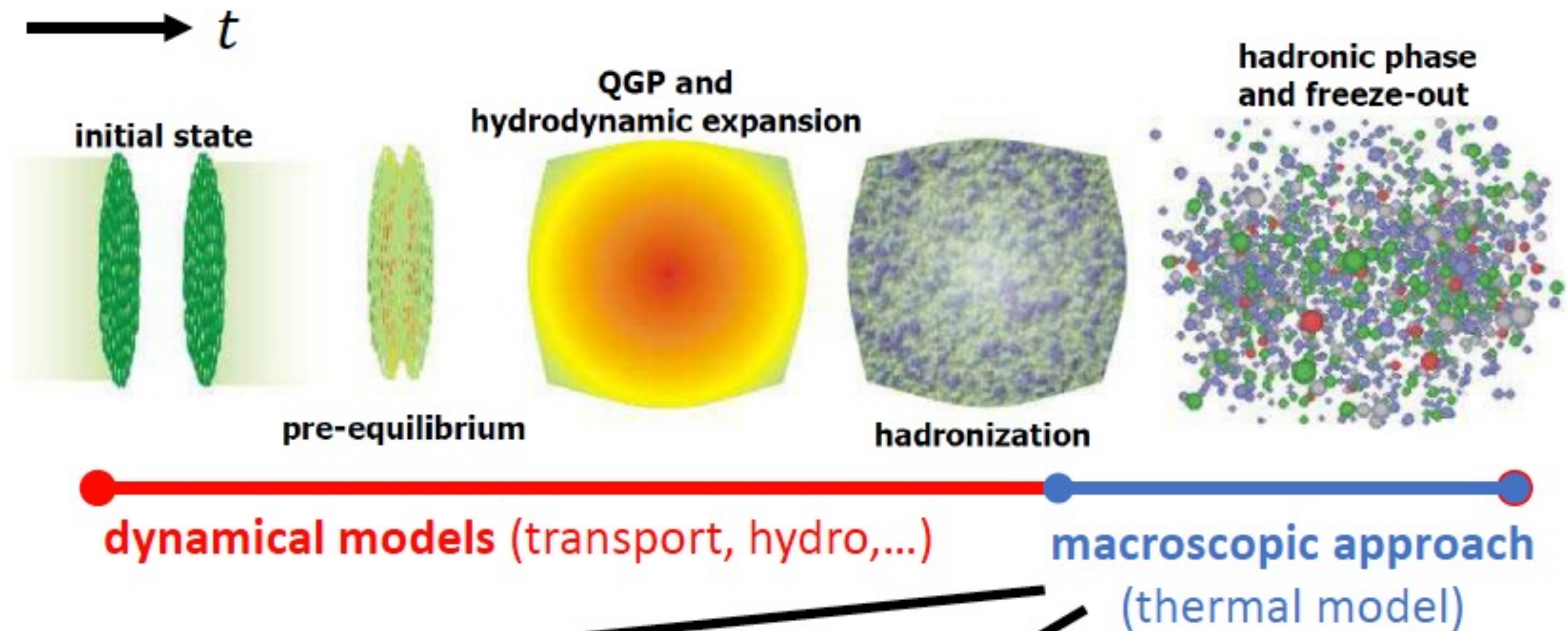

Pros:

- Simplest model with very few free parameters (T, μ_B,...)
- Connection to QCD phase diagram
- Easier to test new ideas

Cons:

- No dynamics
- Describes only yields
- Thermal parameters fitted to data at each energy

Thermal fits at LHC

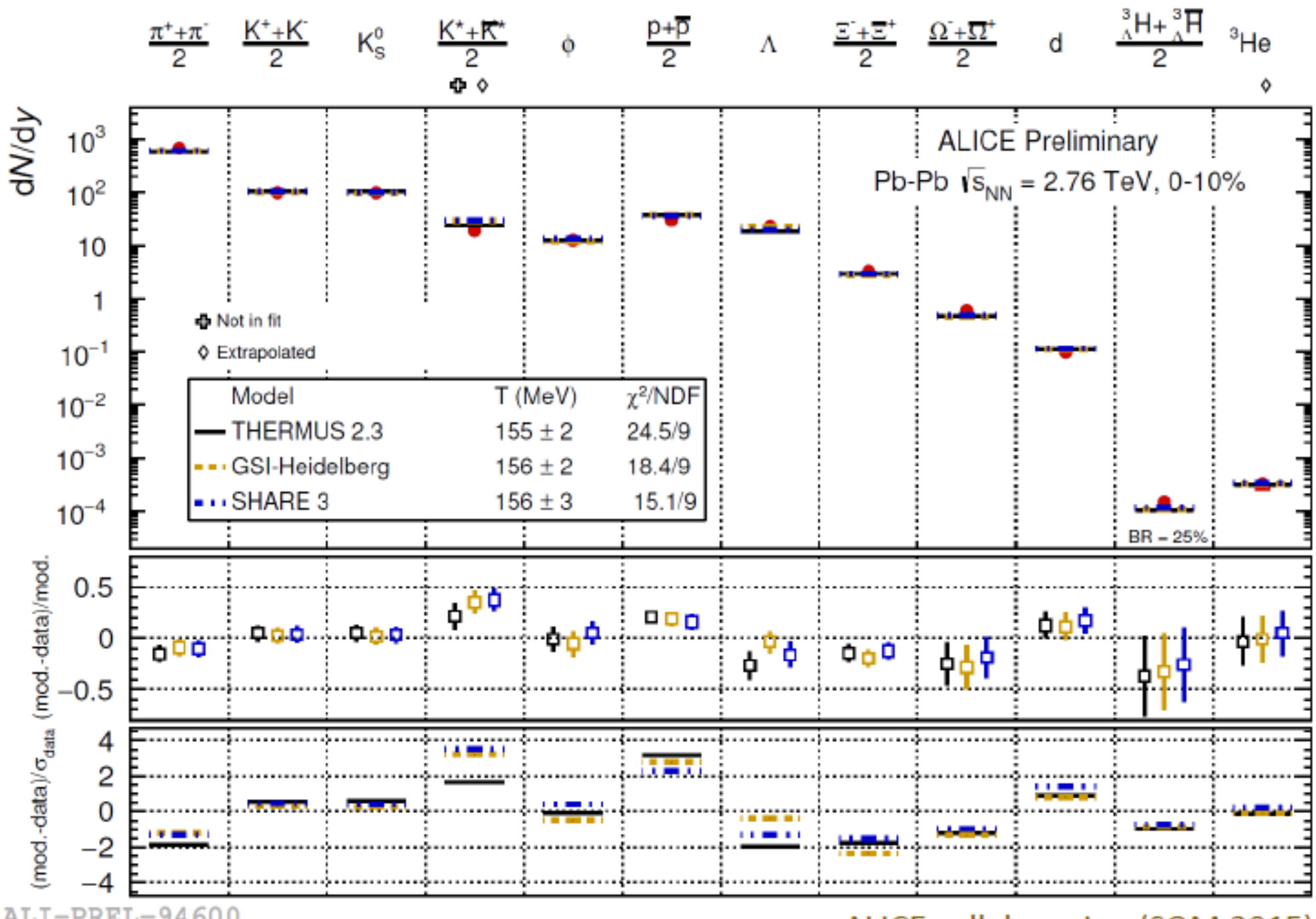

ALICE collaboration (SQM 2015)

BOLTZMANN-GIBBS VS TSALLIS STATISTICS

Boltzmann-Gibbs

$$n_i = \frac{g_i}{(2\pi)^3} \int f(p, m_i) d^3p \,,$$

$$\varepsilon_i = \frac{g_i}{(2\pi)^3} \int \sqrt{p^2 + m_i^2}\, f(p, m_i) d^3p$$

$$f(p, m_i) = \left[\exp\left(\frac{\epsilon_i - \mu_i}{T} \right) \pm 1 \right]^{-1}$$

$$P_i = \frac{g_i}{(2\pi)^3} \int \frac{p^2}{3(p^2 + m_i^2)^{1/2}} f(p, m_i) d^3p$$

$$\mu_i = B_i \mu_{\mathrm{B}} + S_i \mu_{\mathrm{S}}$$

Tsallis

$$N = gV \int \frac{d^3p}{(2\pi)^3} \left[1 + (q-1) \frac{E-\mu}{T} \right]^{-\frac{q}{q-1}} ,$$

$$\epsilon = g \int \frac{d^3p}{(2\pi)^3} E \left[1 + (q-1) \frac{E-\mu}{T} \right]^{-\frac{q}{q-1}} ,$$

$$P = g \int \frac{d^3p}{(2\pi)^3} \frac{p^2}{3E} \left[1 + (q-1) \frac{E-\mu}{T} \right]^{-\frac{q}{q-1}}$$

if q=1 then BG statistics is restored

J. Cleymans et al., PLB 723 (2013) 351

EXAMPLE: PROTON-PROTON COLLISIONS

CMS Collab., JHEP 08 (2011) 086

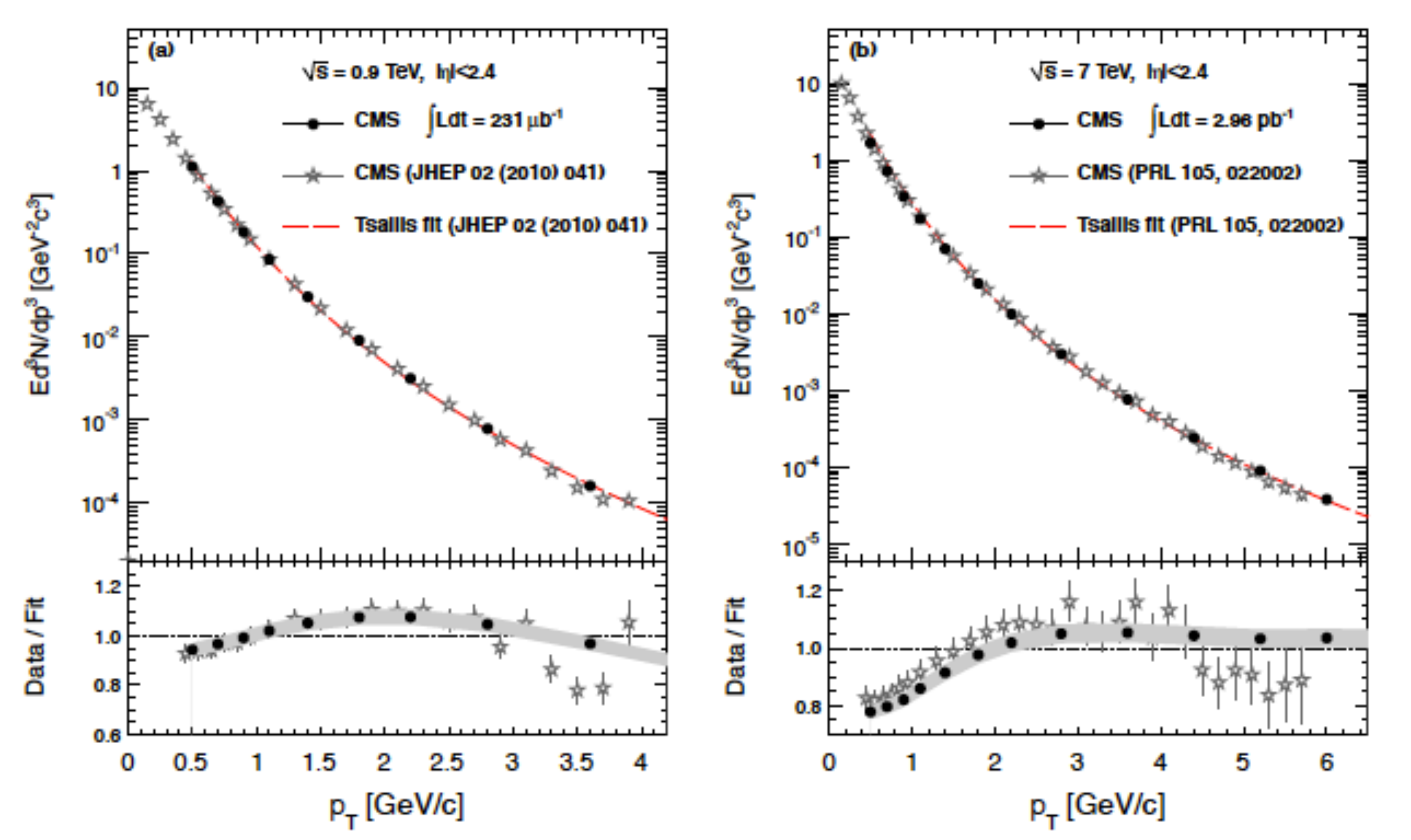

Models: UrQMD, SMASH

HICs at intermediate energies

INITIAL PARTICLE PRODUCTION IN URQMD

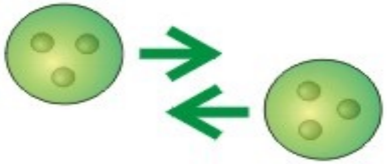

- in high energy collisions hadrons can be excited into *strings*
- a *color flux-tube* is formed by pulling one valence quark away from the remaining ones in the hadron

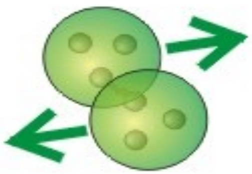

- if the color-field increases beyond a critical value (defined by the *string-tension*), spontaneous quark-antiquark creation from the *Dirac sea* occurs (*Schwinger mechanism*)

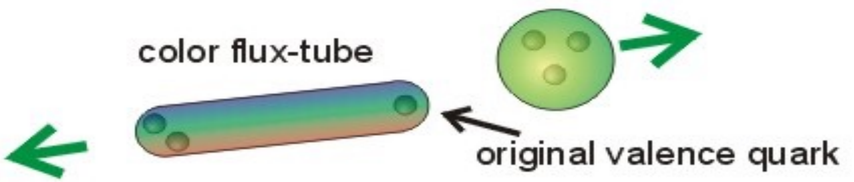

- newly created (anti-)quarks require a *formation time* to form hadrons

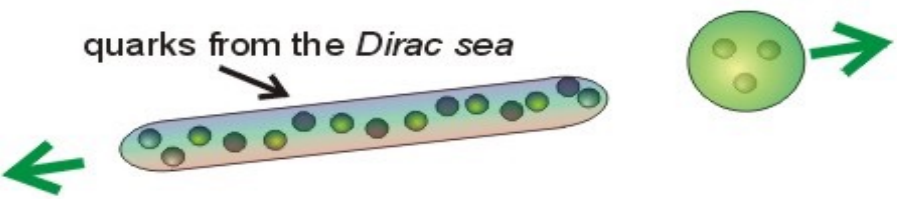

- *leading hadrons* interact with *reduced cross sections* during their formation time

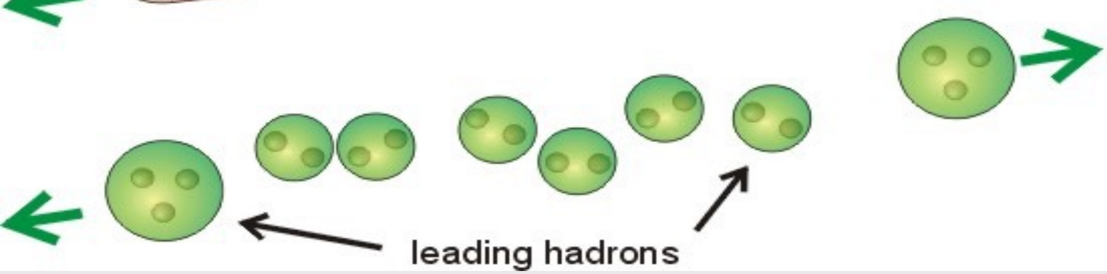

- *newly created hadrons* have *zero cross section* during their formation time

S. Bass et al., Prog.Part.Nucl.Phys. 41 (1998) 255
M. Bleicher, E.Z., et al., J.Phys.G 25 (1999) 1859

SMASH: general properties J. Weil *et al.*, Phys.Rev. C94 (2016) no.5, 054905

- Monte-Carlo solver of relativistic Boltzmann equations
  BUU type approach, testparticles ansatz: $N \to N \cdot N_{test}$, $\sigma \to \sigma / N_{test}$
- Degrees of freedom
  - most of established hadrons from PDG up to mass 2.5 GeV
  - strings: do not propagate, only form and decay to hadrons
  - leptons and photons production, decoupled from hadronic evolution
- Propagate from action to action (timesteps only for potentials)
  action $\equiv$ collision, decay, wall crossing
- Geometrical collision criterion: $d_{ij} \leq \sqrt{\sigma/\pi}$
- Interactions: $2 \leftrightarrow 2$ and $2 \to 1$ collisions, decays, potentials, string formation (soft - SMASH, hard - Pythia 8) and fragmentation via Pythia 8
- C++ code, git version control, public on github

EVOLUTION OF TEMPERATURE T AND ENERGY DENSITY ε

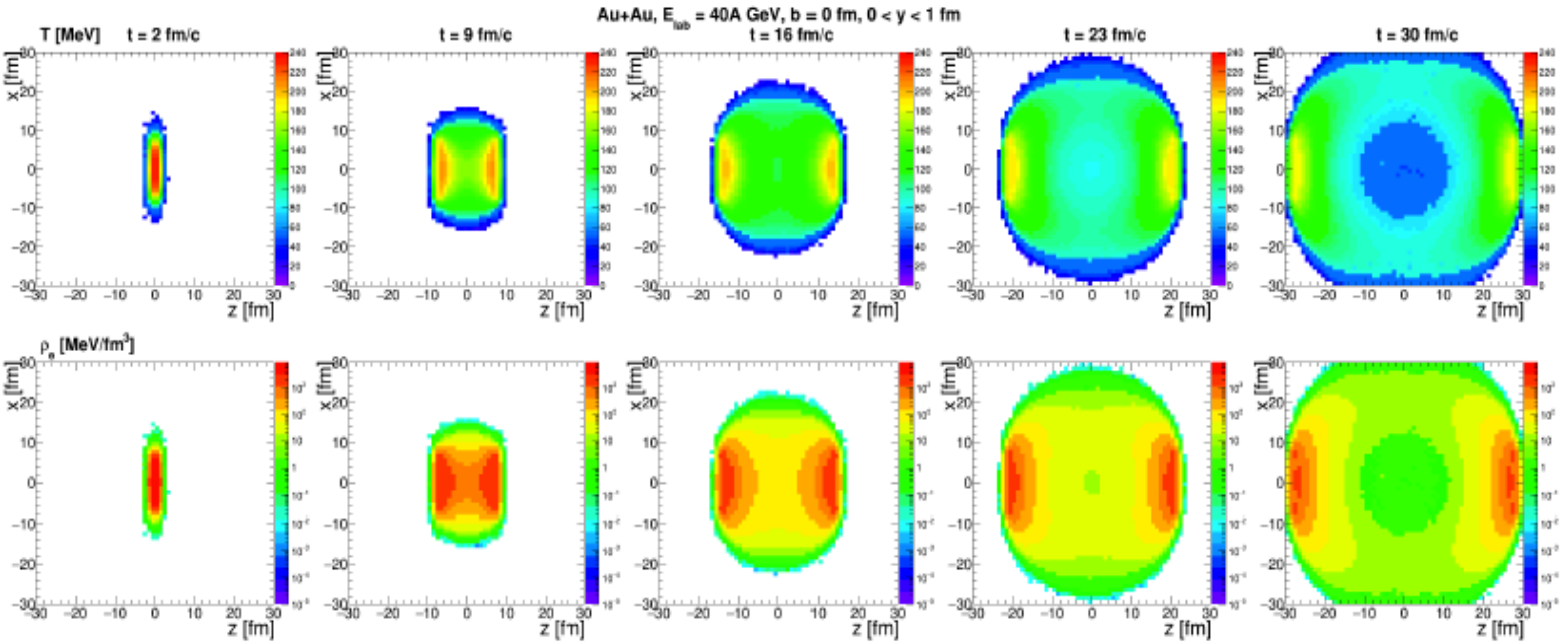

There is no global equilibrium in the whole volume of the fireball.
We opted for the central cell with volume $V = 5{\times}5{\times}5 = 125\ fm^3$

EVOLUTION OF BARYON CHEMICAL POTENTIAL μ_B AND NET-BARYON DENSITY ρ_B

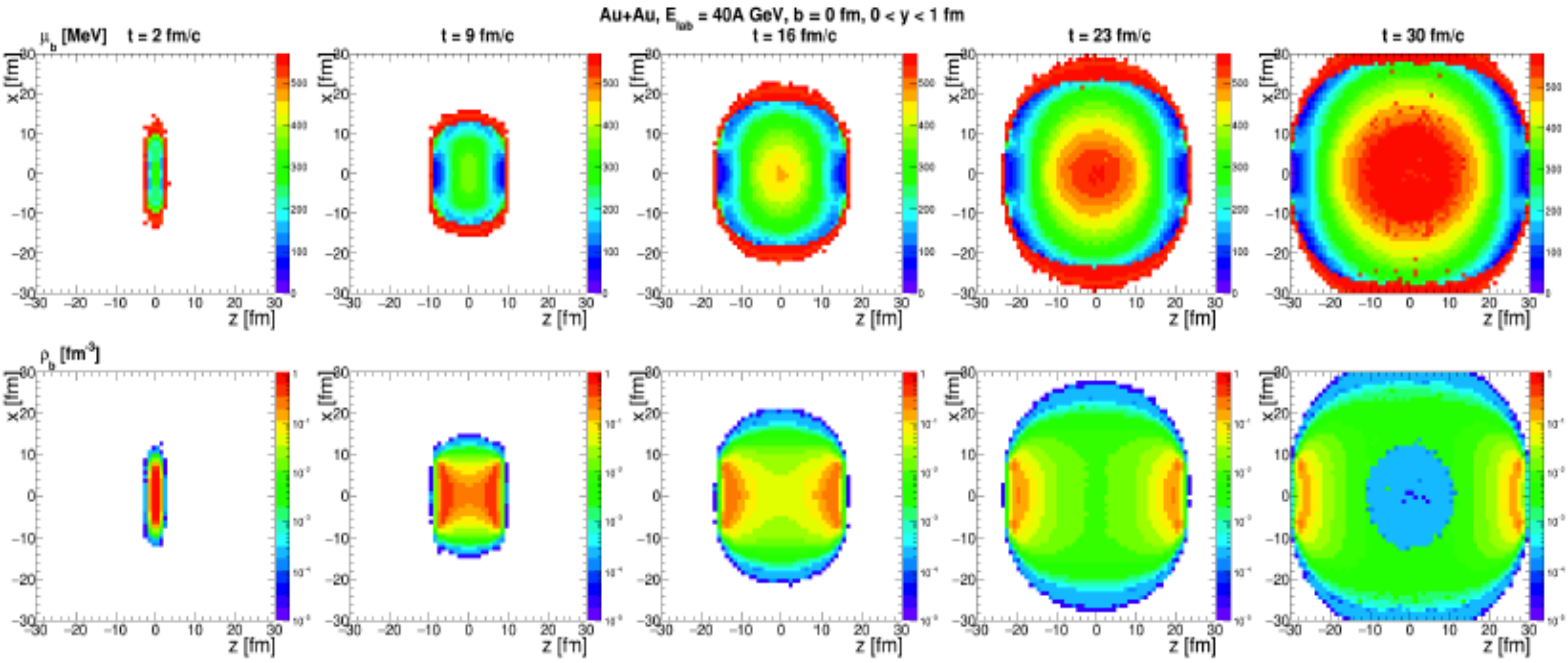

Net-baryon density is non-uniformly distributed within the whole volume, therefore baryon chemical potential is also different in different areas

EVOLUTION OF STRANGENESS CHEMICAL POTENTIAL μ_S AND NET-STRANGENESS DENSITY ρ_S

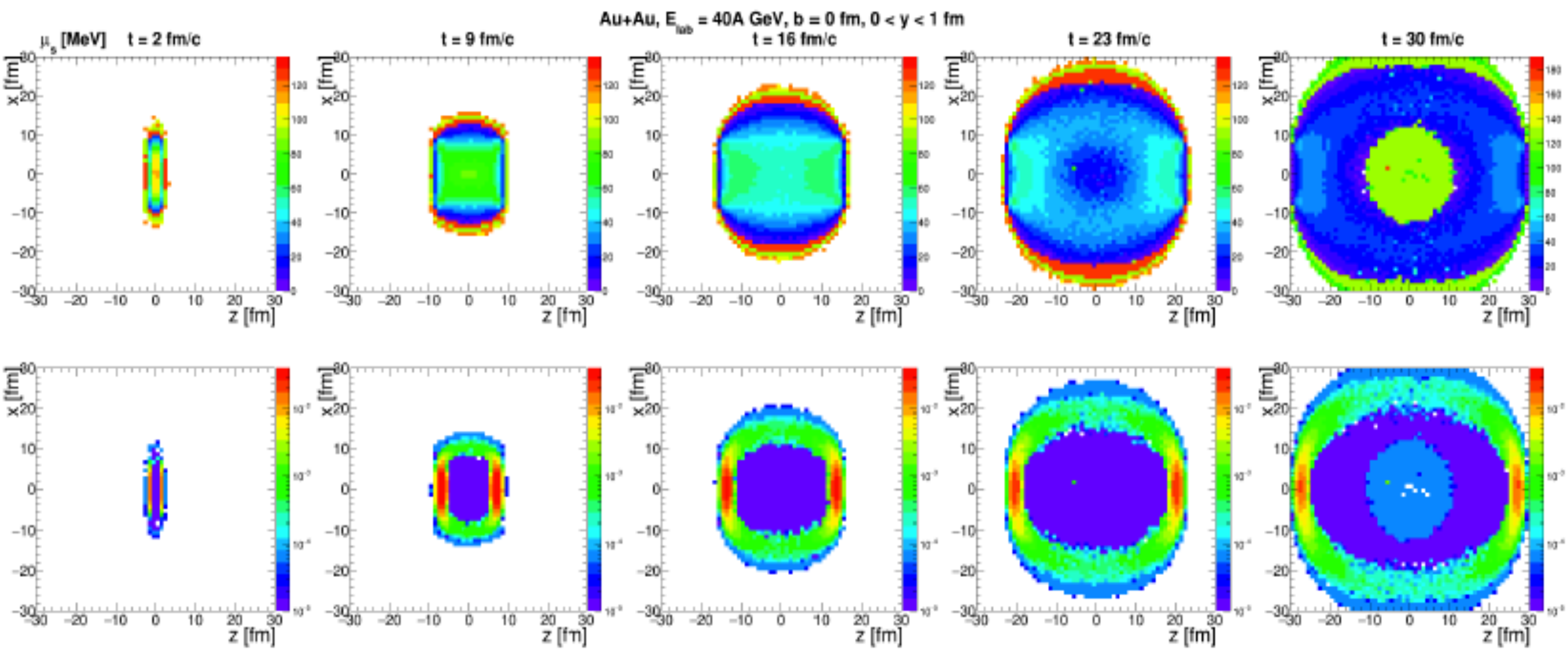

Net-strangeness density is also non-uniformly distributed within the whole volume.
Net-strangeness chemical potential is different in different areas

Central cell and

Box with periodic boundary conditions

Equilibration in the Central Cell

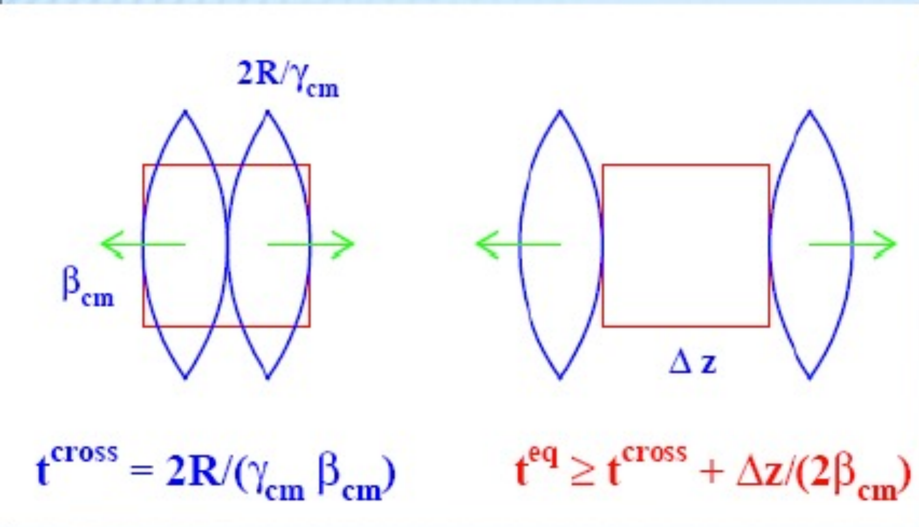

Kinetic equilibrium:

Isotropy of velocity distributions

Isotropy of pressure

Thermal equilibrium:

Energy spectra of particles are described by Boltzmann distribution

L.Bravina et al., PLB 434 (1998) 379; JPG 25 (1999) 351

$$\frac{dN_i}{4\pi pEdE} = \frac{Vg_i}{(2\pi\hbar)^3}\exp\left(\frac{\mu_i}{T}\right)\exp\left(-\frac{E_i}{T}\right)$$

Chemical equlibrium:

Particle yields are reproduced by SM with the same values of $(T,\ \mu_B,\ \mu_S)$:

$$N_i = \frac{Vg_i}{2\pi^2\hbar^3}\int_0^\infty p^2dp\exp\left(\frac{\mu_i}{T}\right)\exp\left(-\frac{E_i}{T}\right)$$

THERMAL AND CHEMICAL EQUILIBRIUM

Boltzmann fit to the energy spectra **Particle yields**

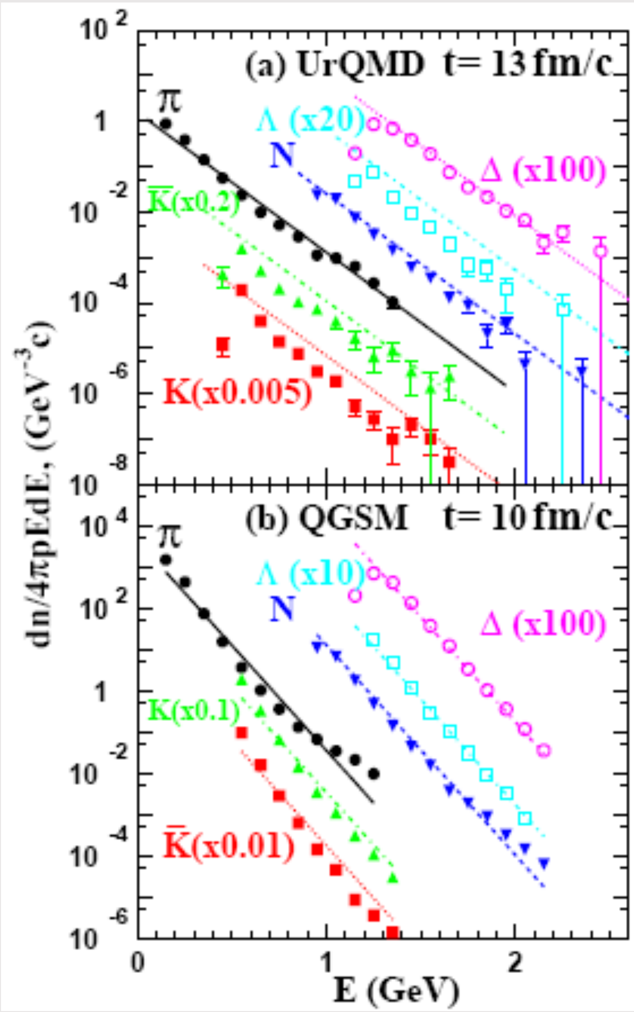

L.Bravina et al., PRC 78, 014907 (2008)

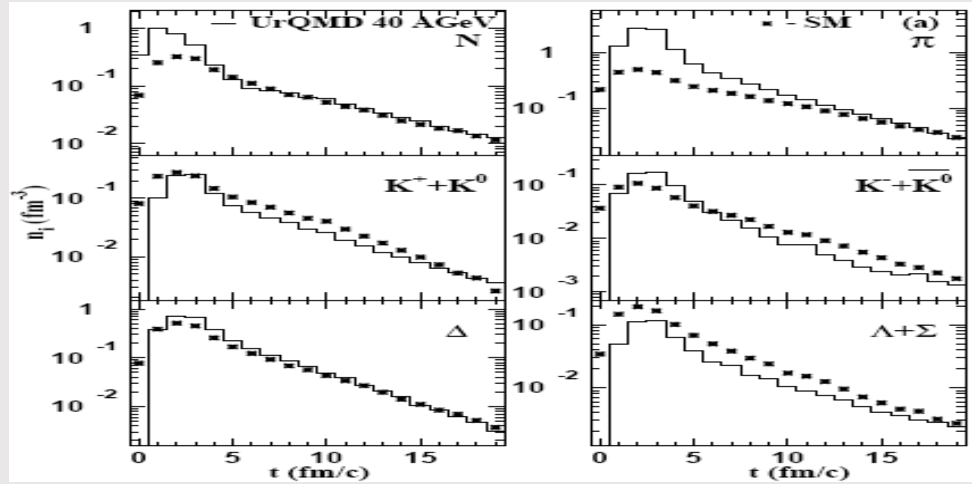

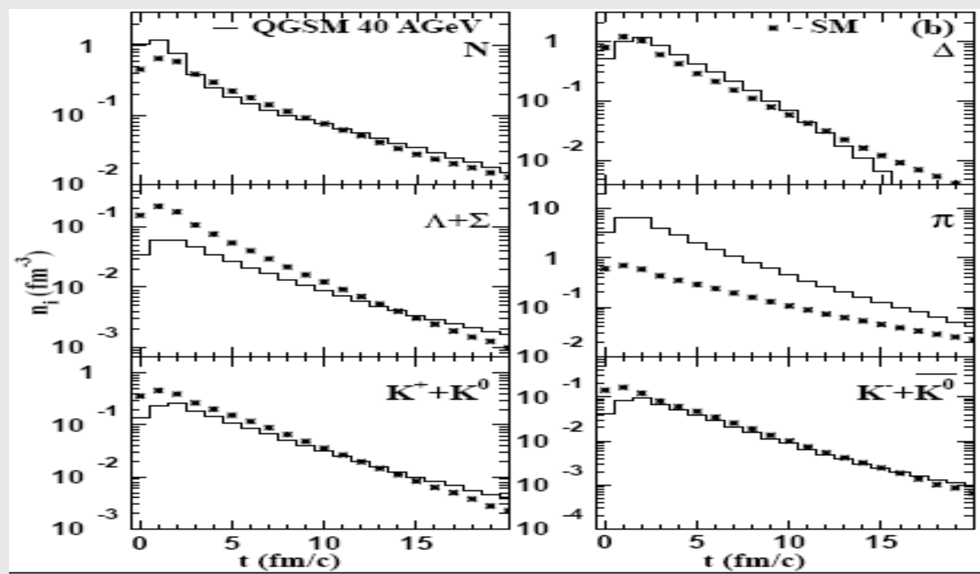

Thermal and chemical equilibrium seems to be reached

Box with periodic boundary conditions

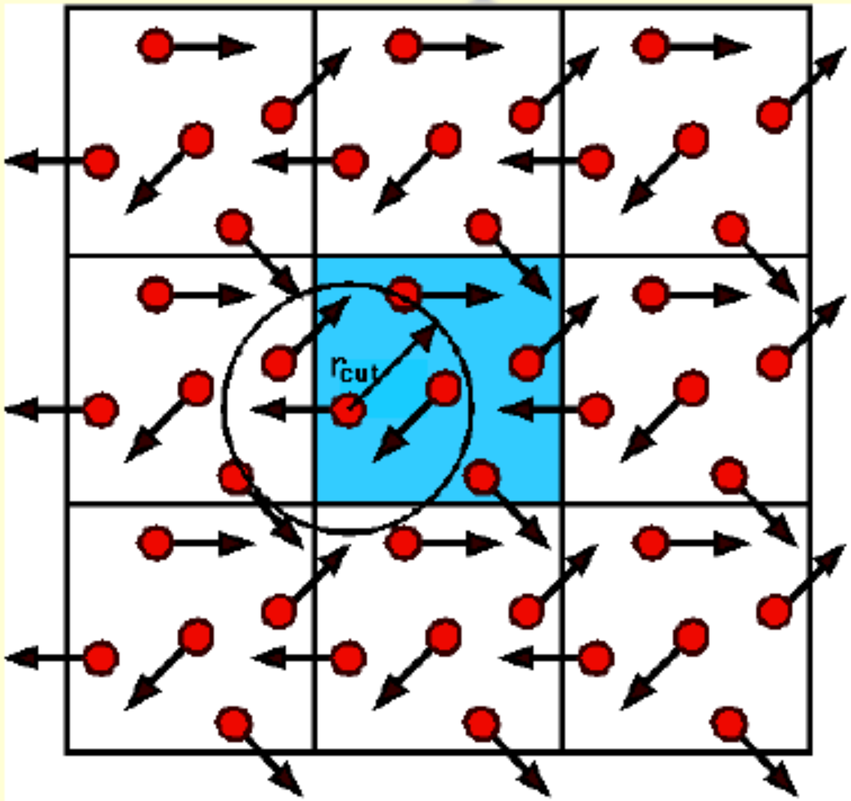

M.Belkacem et al., PRC 58, 1727 (1998)

Model employed: UrQMD
55 different baryon species
(N, Δ, hyperons and their
resonances with
$m \leq 2.25$ GeV/c^2)
32 different meson species
(including resonances with
$m \leq 2$ GeV/c^2) and their
respective antistates.
For higher mass excitations
a string mechanism is invoked.

Initialization: (i) nucleons are uniformly distributed in a configuration space;
(ii) Their momenta are uniformly distributed in a sphere with random radius and then rescaled to the desired energy density.

Test for equilibrium: particle yields and energy spectra

BOX: PARTICLE ABUNDANCES

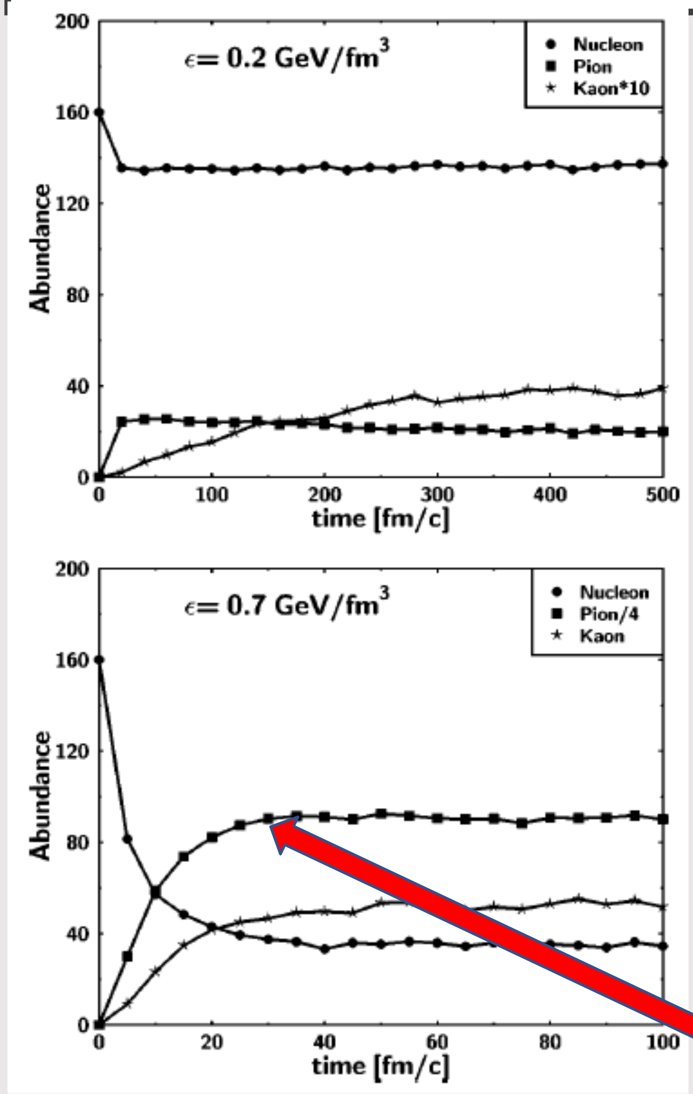

M.Belkacem et al., PRC 58, 1727 (1998)

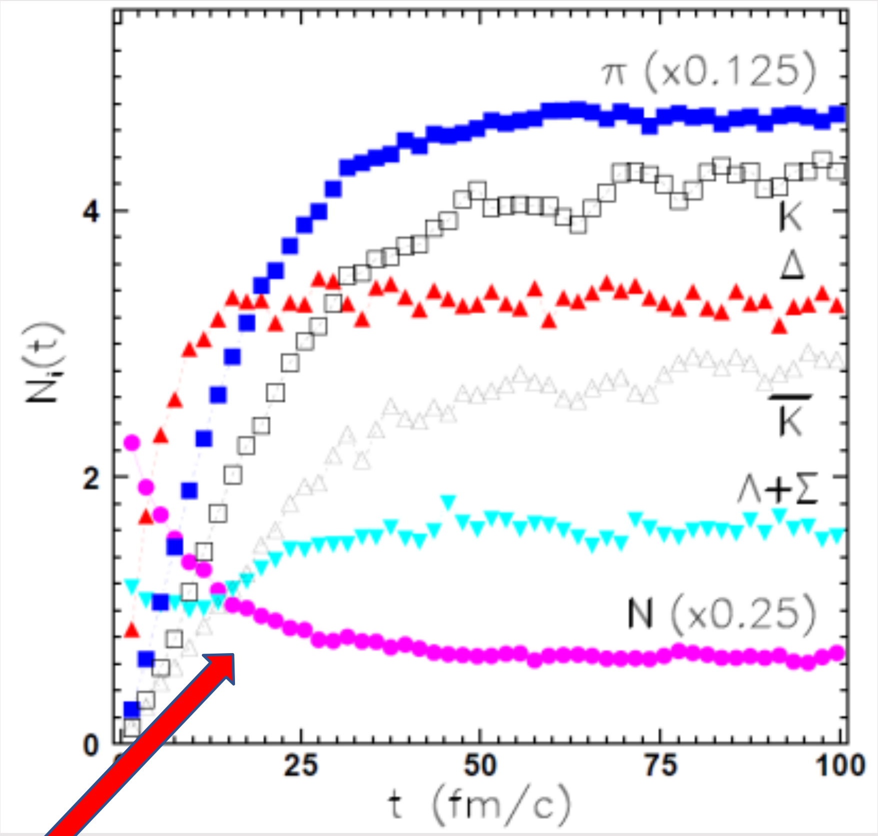

L.Bravina et al., PRC 62, 064906 (2000)

Saturation of yields after a certain time. Strange hadrons are saturated longer compared to other hadrons

Results for central

Au+Au collisions

TSALLIS FIT VS BOLTZMANN FIT

Pions, Au+Au central collisions at $\sqrt{s} = 4$ GeV and 7.7 GeV

CELL (UrQMD)

BOX (SMASH)

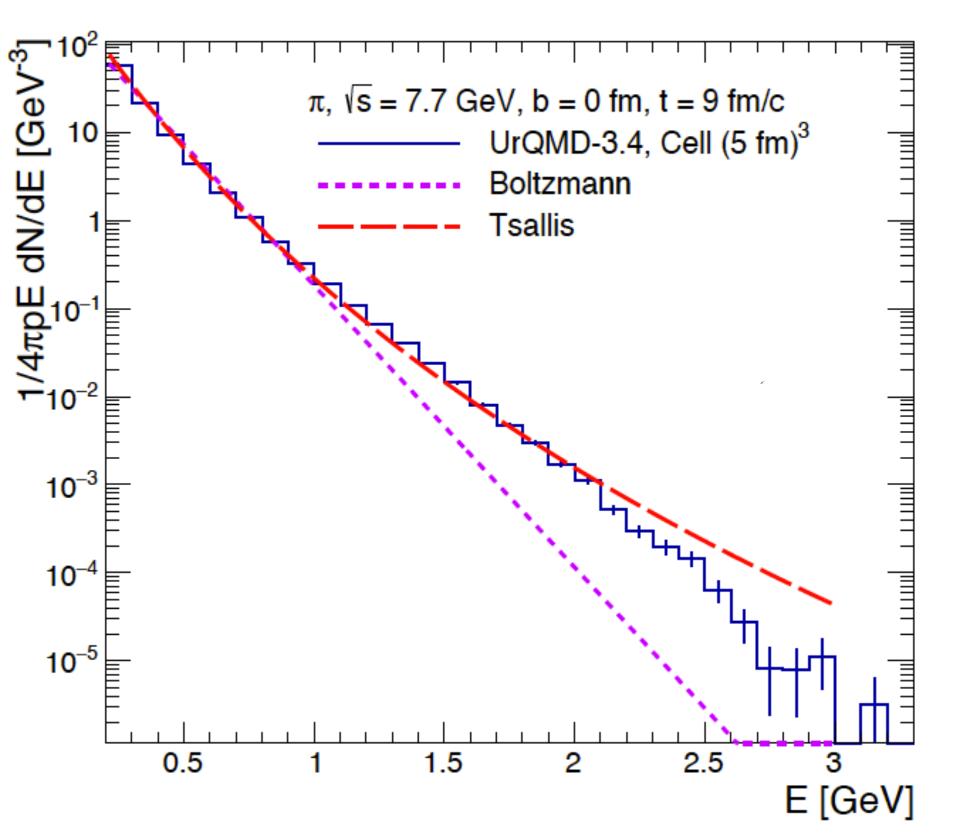

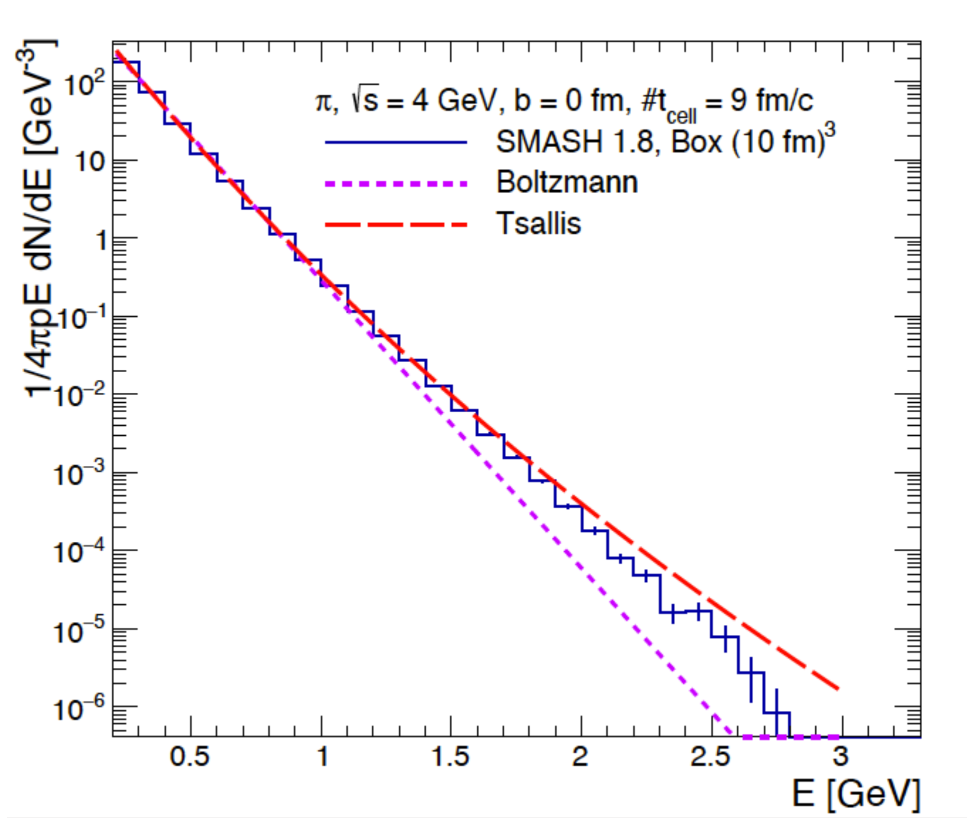

Deviations from BG distribution for cell and box spectra in both models

TSALLIS FIT VS BOLTZMANN FIT

Au+Au central collisions at $\sqrt{s} = 4$ GeV (UrQMD)

CELL

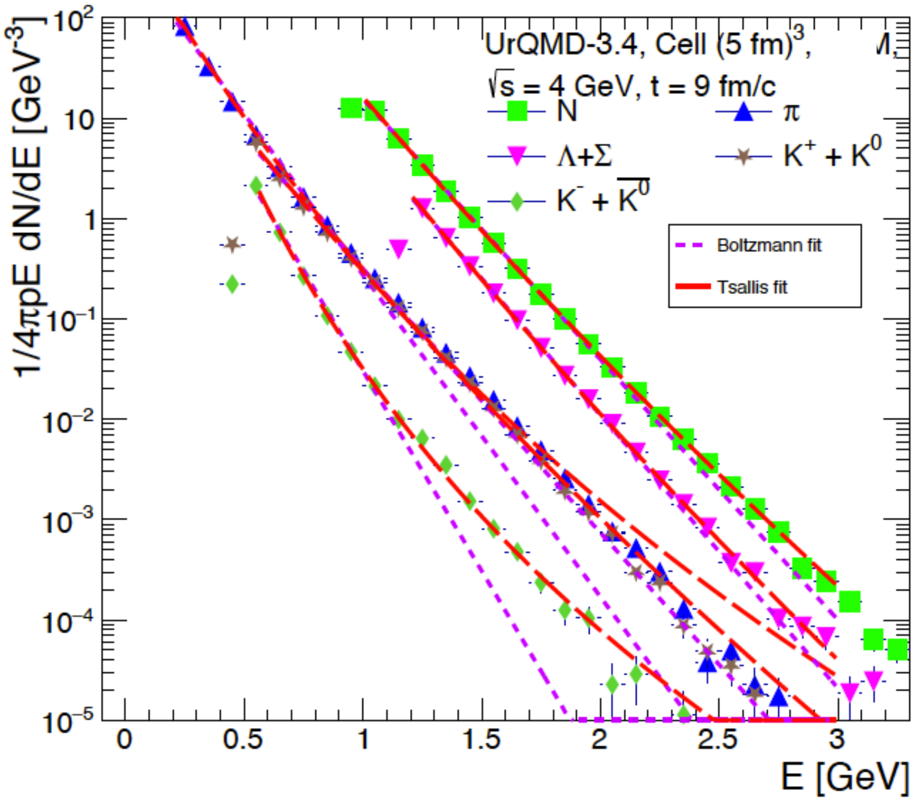

BOX

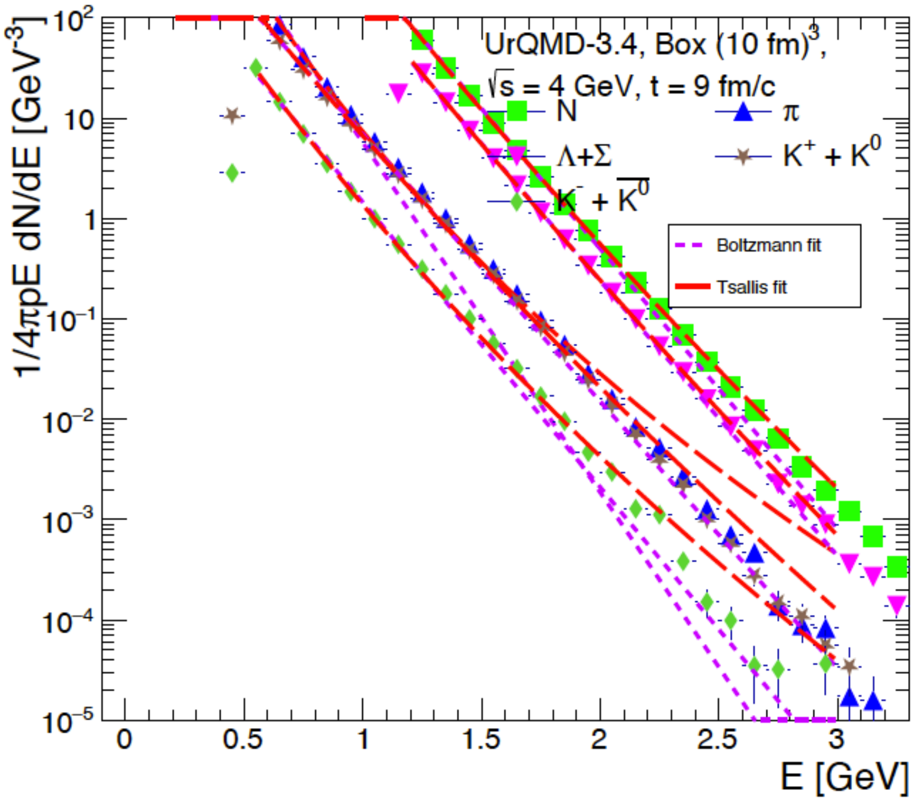

Tsallis distribution better matches the particle spectra both for the matter in the cell and for the infinite nuclear matter

TIME EVOLUTION OF Q IN THE CELL

Au+Au central collisions at $\sqrt{s} = 4$ GeV and 7.7 GeV

UrQMD 3.4

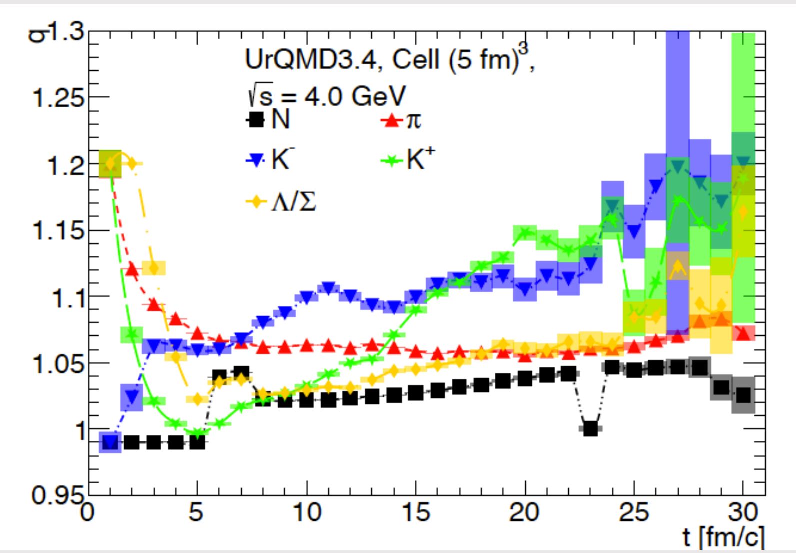

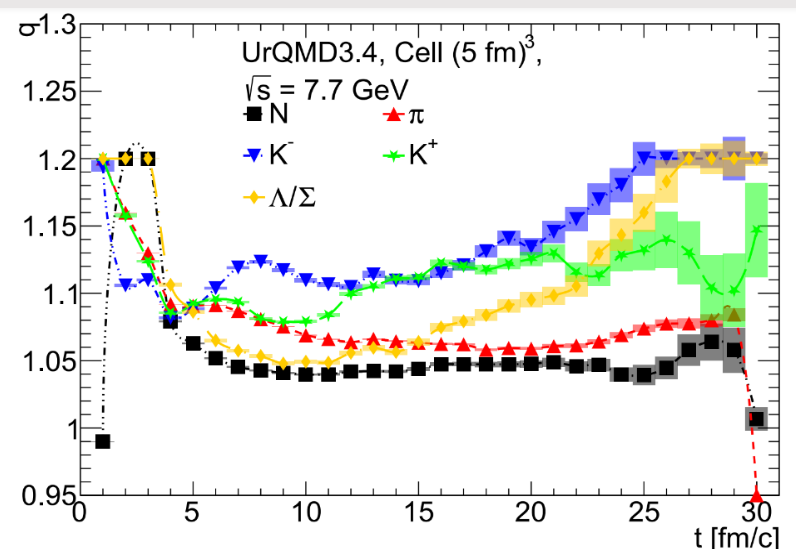

q varies from 1.02 to 1.15

SMASH 2.2

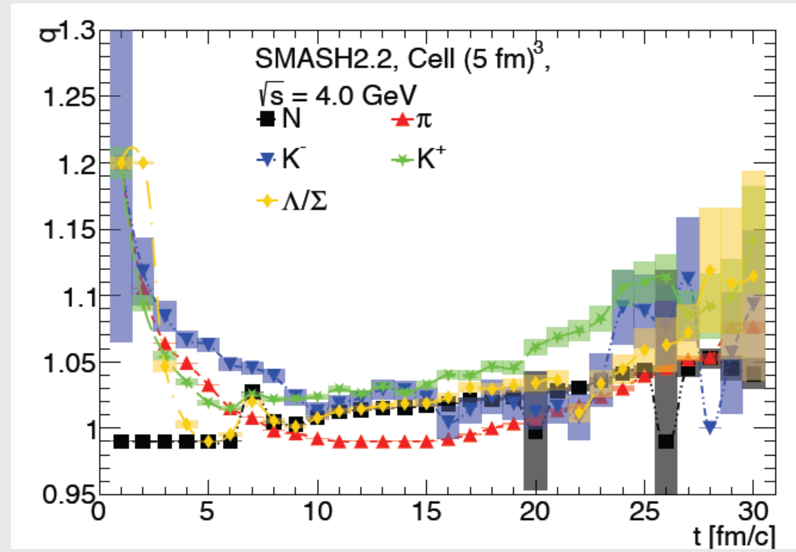

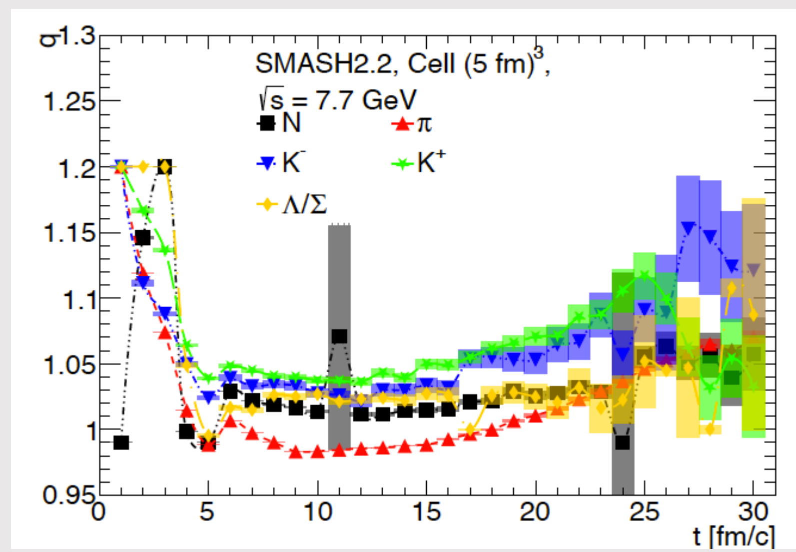

q varies slightly, $0.99 < q < 1.07$

TIME EVOLUTION OF q IN THE BOX

Au+Au central collisions at $\sqrt{s} = 4$ GeV and 7.7 GeV

UrQMD 3.4

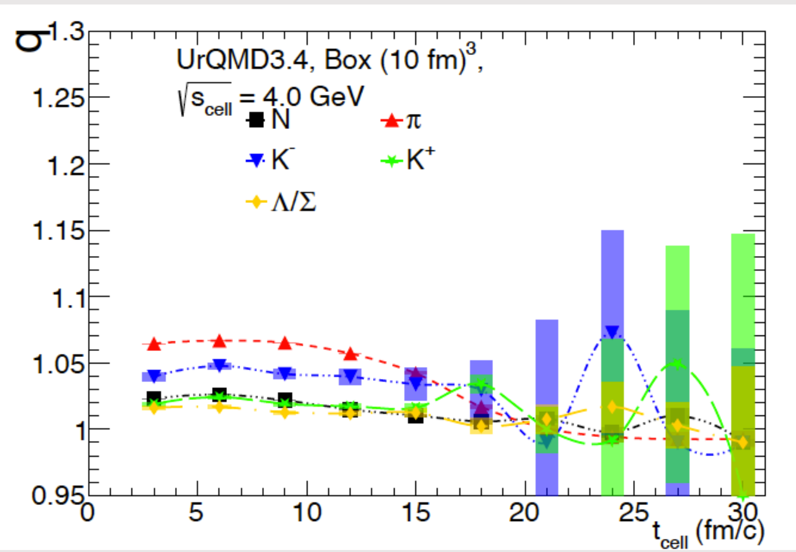

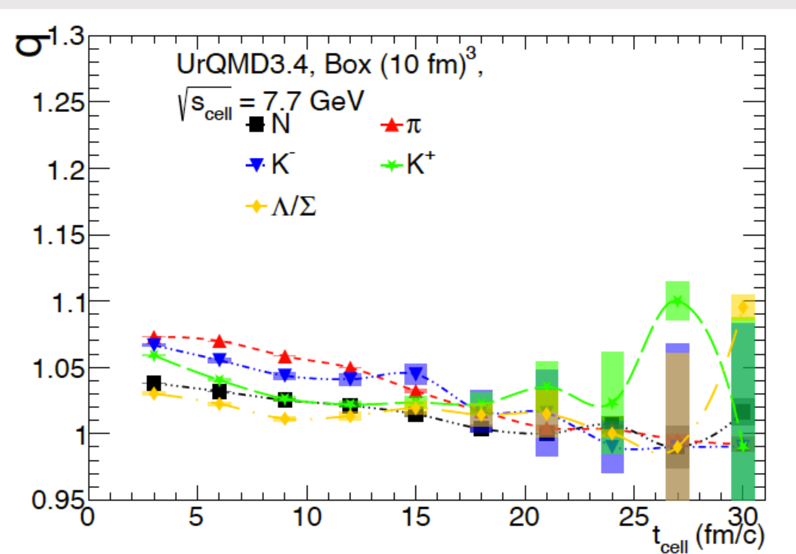

SMASH 2.2

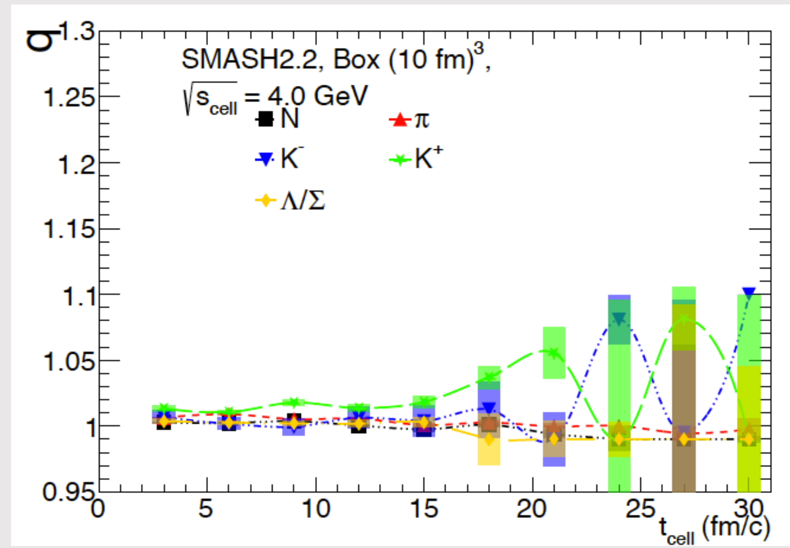

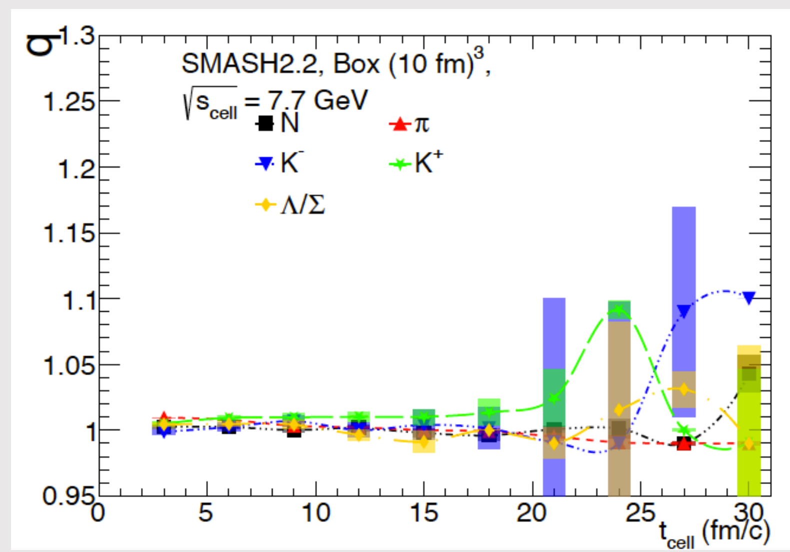

$q > 0$ for times $t_{cell} < 20$ fm/c

q is approximately unity for all times

Q IN THE CELL VS Q IN THE BOX

Au+Au central collisions at $\sqrt{s} = 4$ GeV (UrQMD)

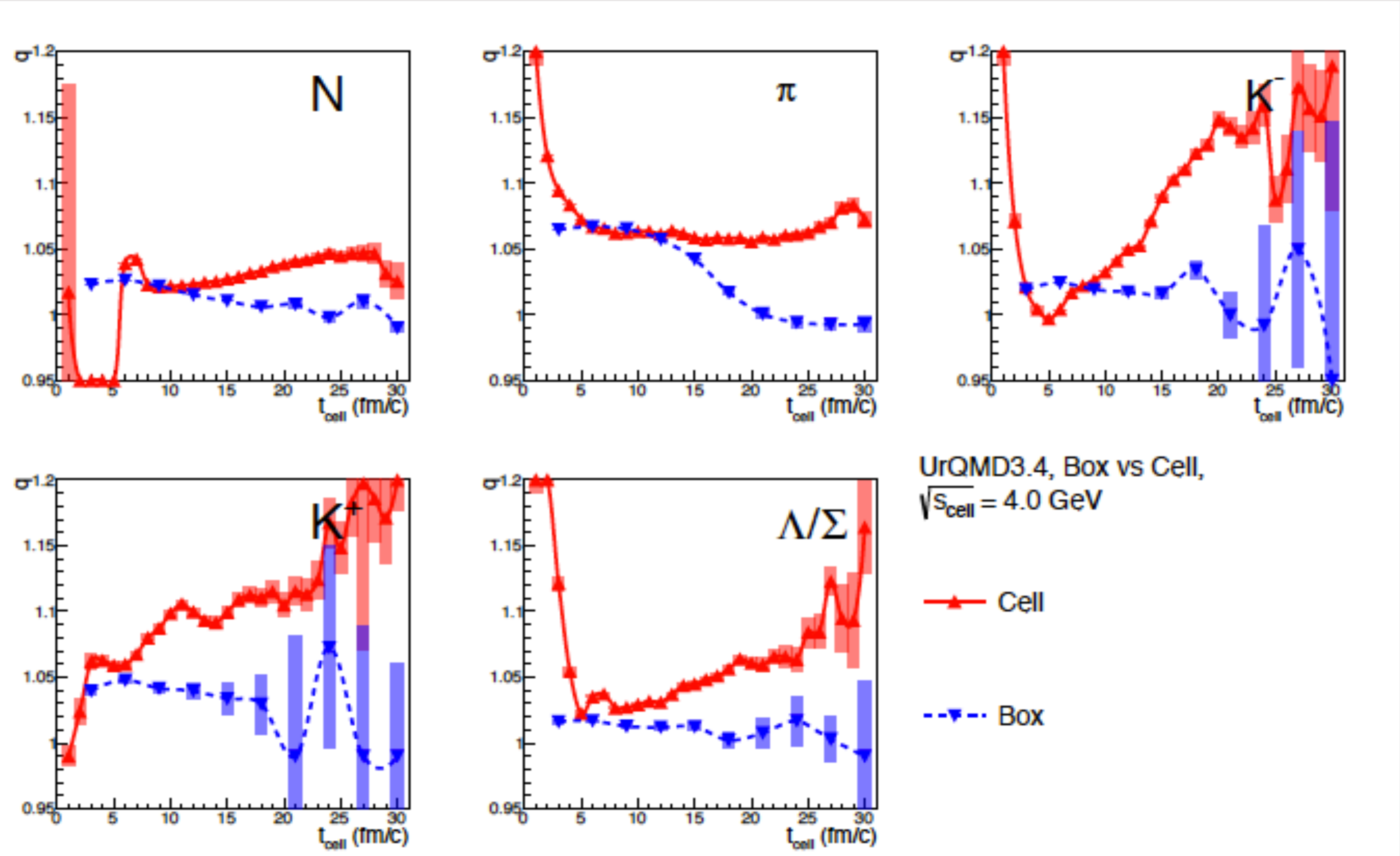

The matter in the cell is close to (albeit not in) equilibrium

Q IN THE CELL VS Q IN THE BOX

Au+Au central collisions at $\sqrt{s} = 4$ GeV (SMASH)

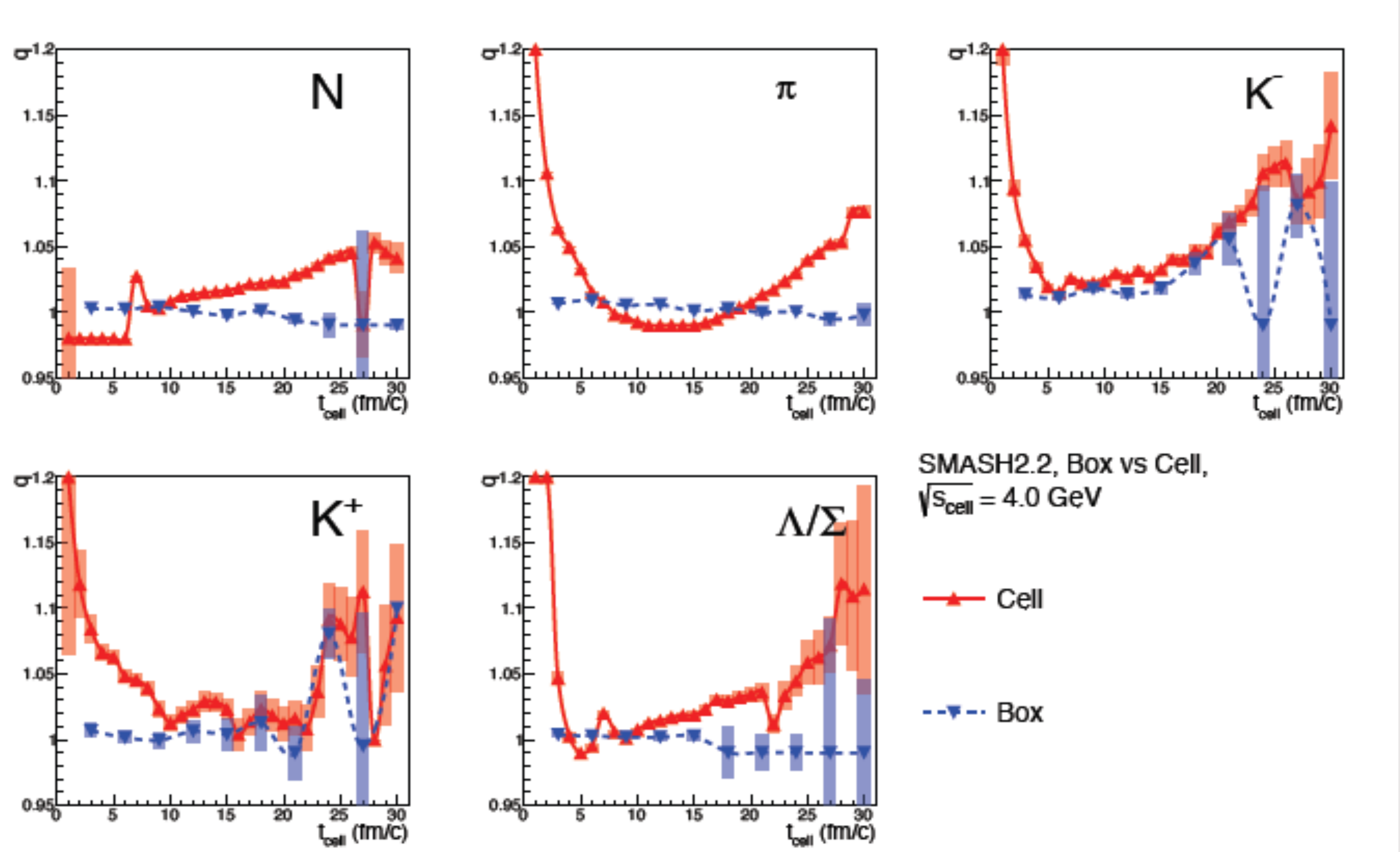

Fair agreement between the cell and the box results

Q IN THE CELL VS Q IN THE BOX

Au+Au central collisions at $\sqrt{s} = 7.7$ GeV (SMASH)

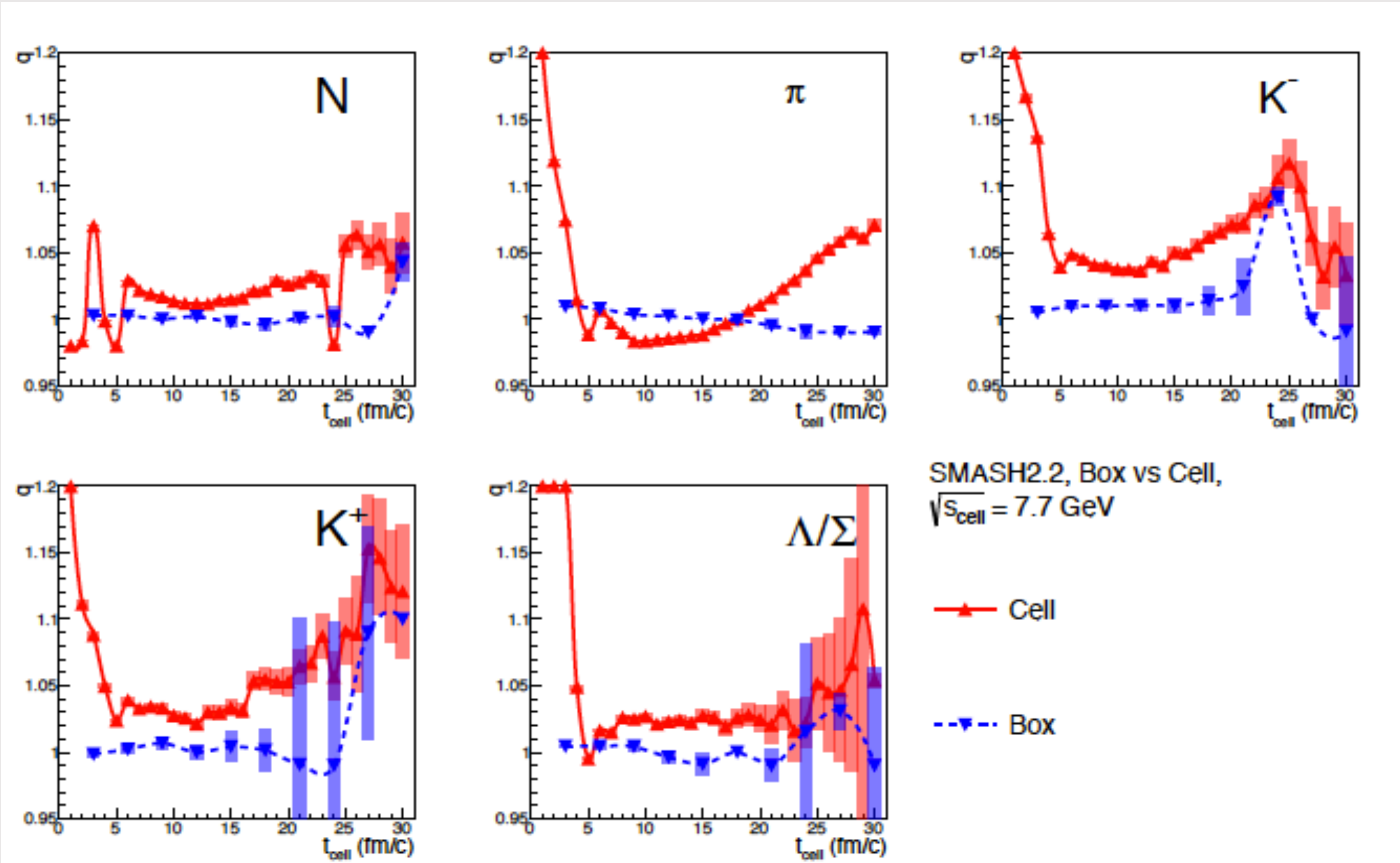

… but for higher energy the agreement is not so good

Q IN THE CELL VS Q IN THE BOX

Au+Au central collisions at $\sqrt{s} = 7.7$ GeV (UrQMD)

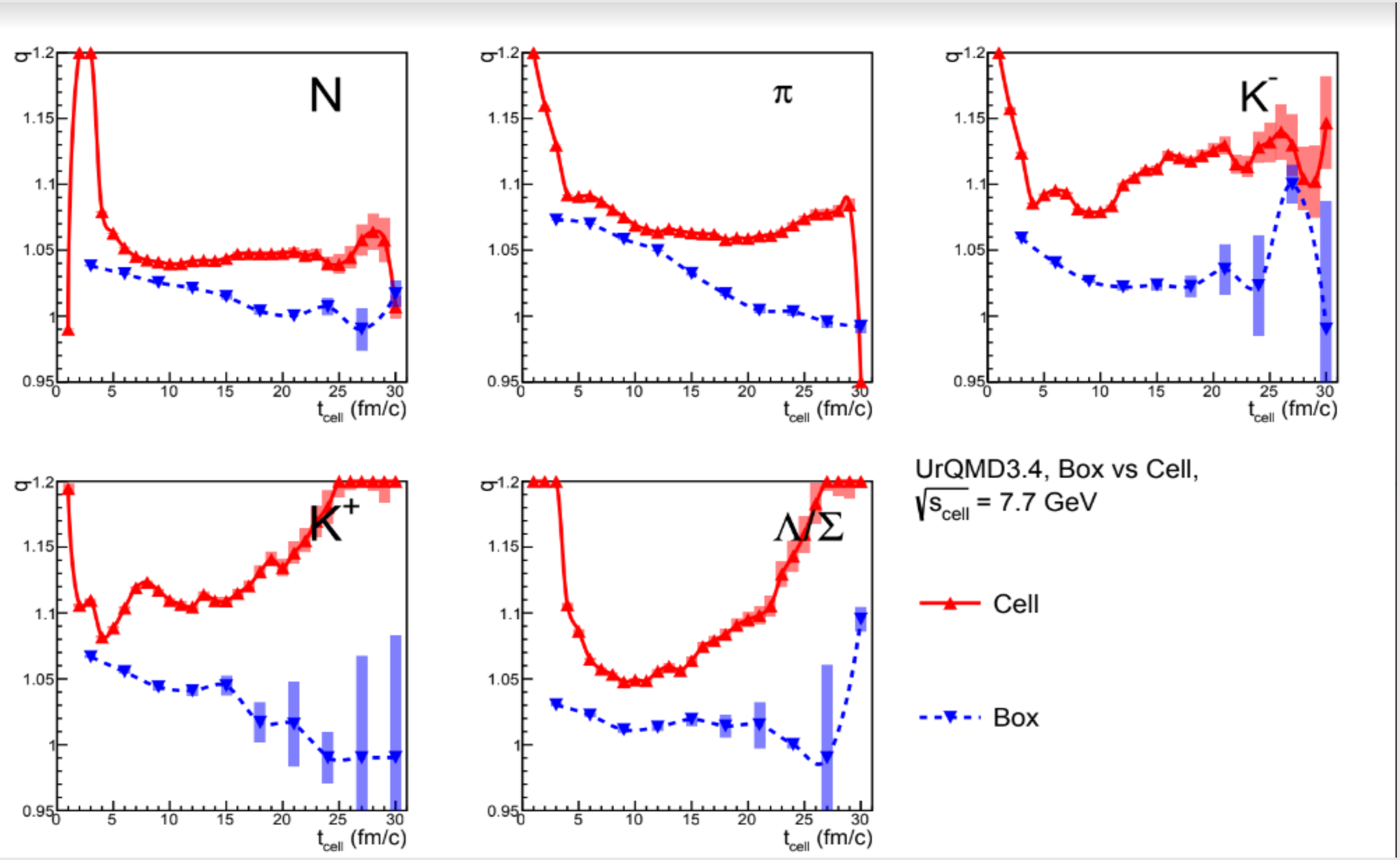

Cell results are not close to the box ones anymore

T IN THE CELL VS *T* IN THE BOX

Au+Au central collisions at $\sqrt{s} = 4$ GeV (UrQMD)

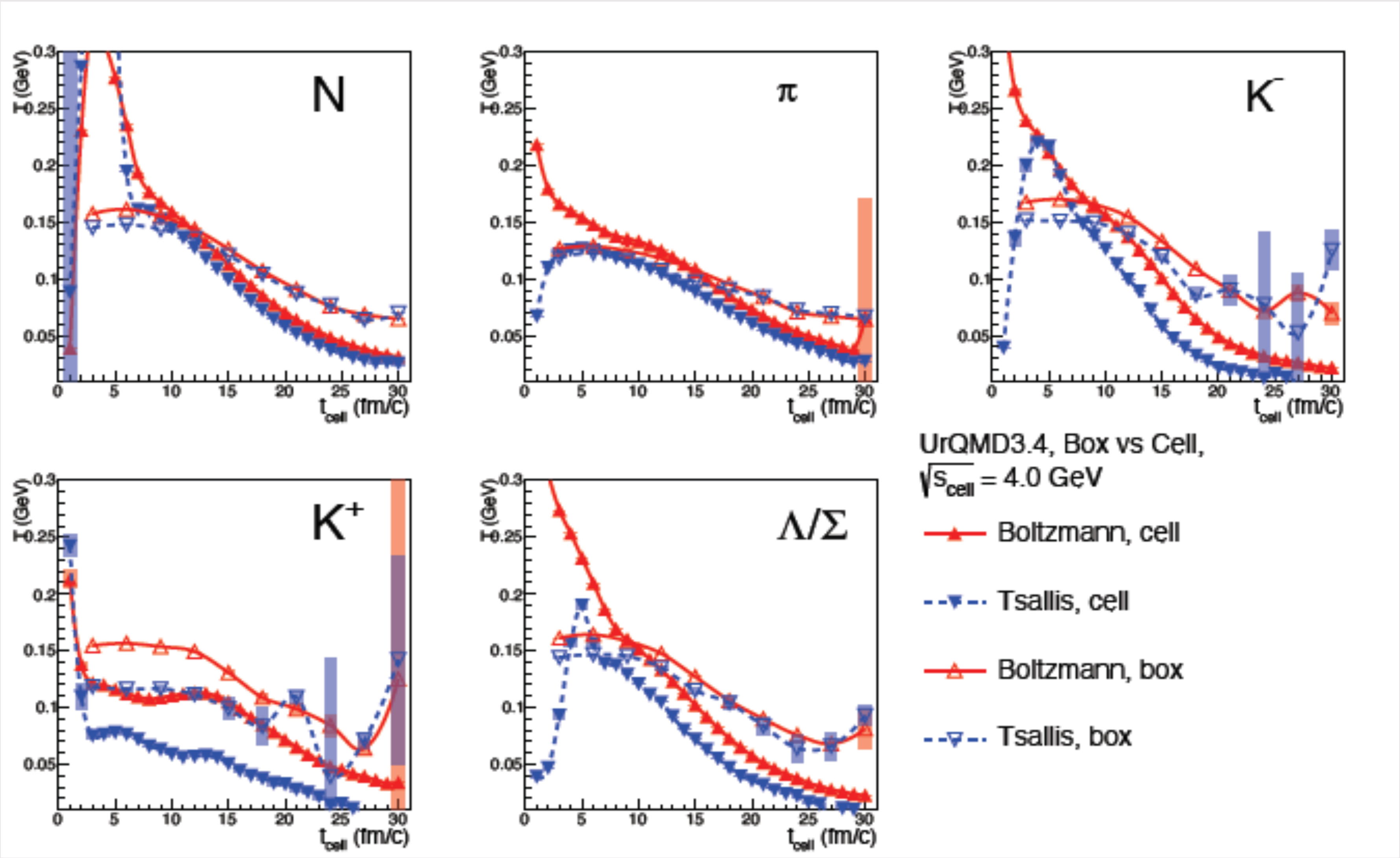

The Tsallis fit provides lower temperatures than the Boltzmann fit

T IN THE CELL VS *T* IN THE BOX

Au+Au central collisions at $\sqrt{s} = 4$ GeV (SMASH)

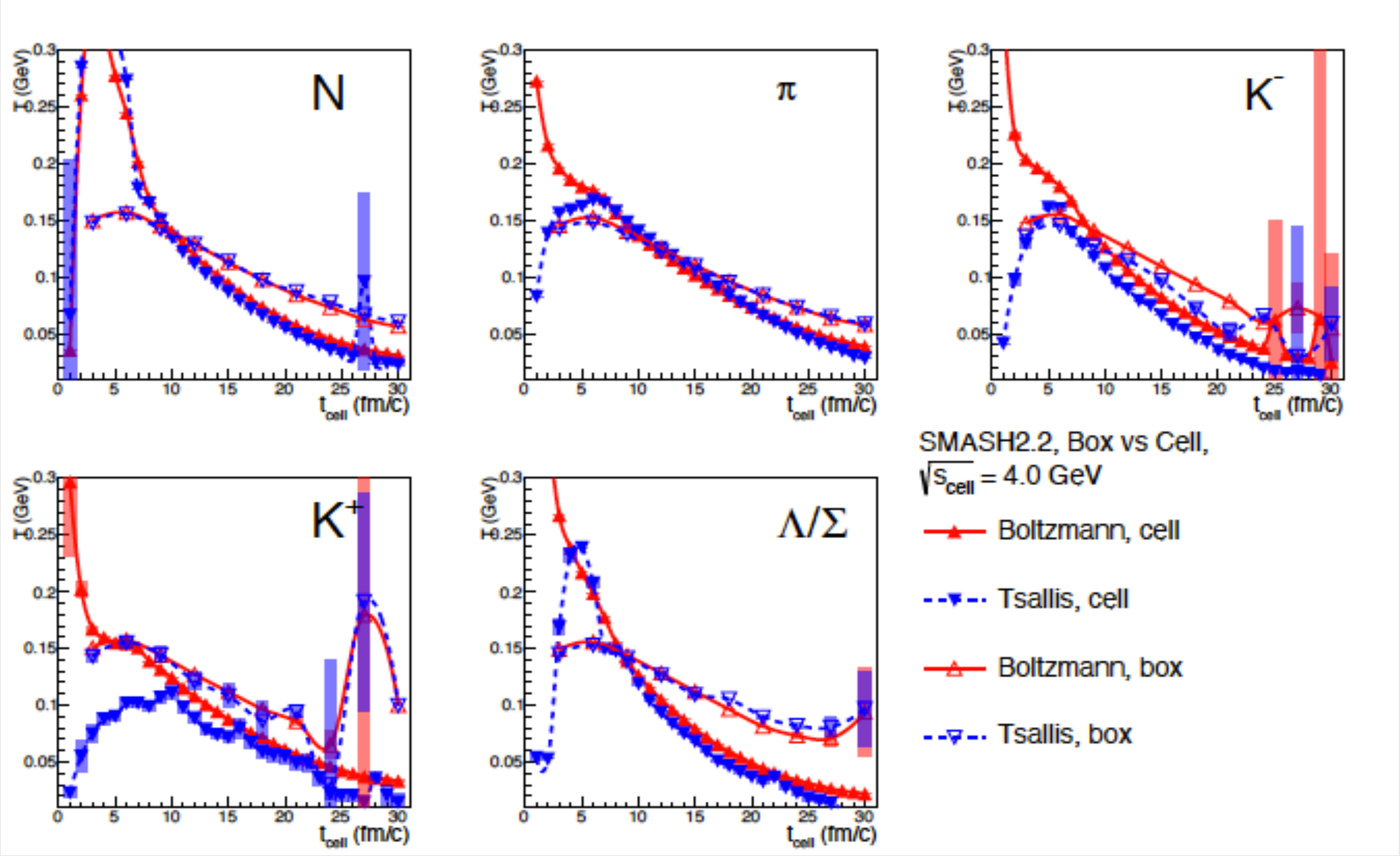

Temperatures of both fits are close to each other

T IN THE CELL VS *T* IN THE BOX

Au+Au central collisions at $\sqrt{s} = 7.7$ GeV (SMASH)

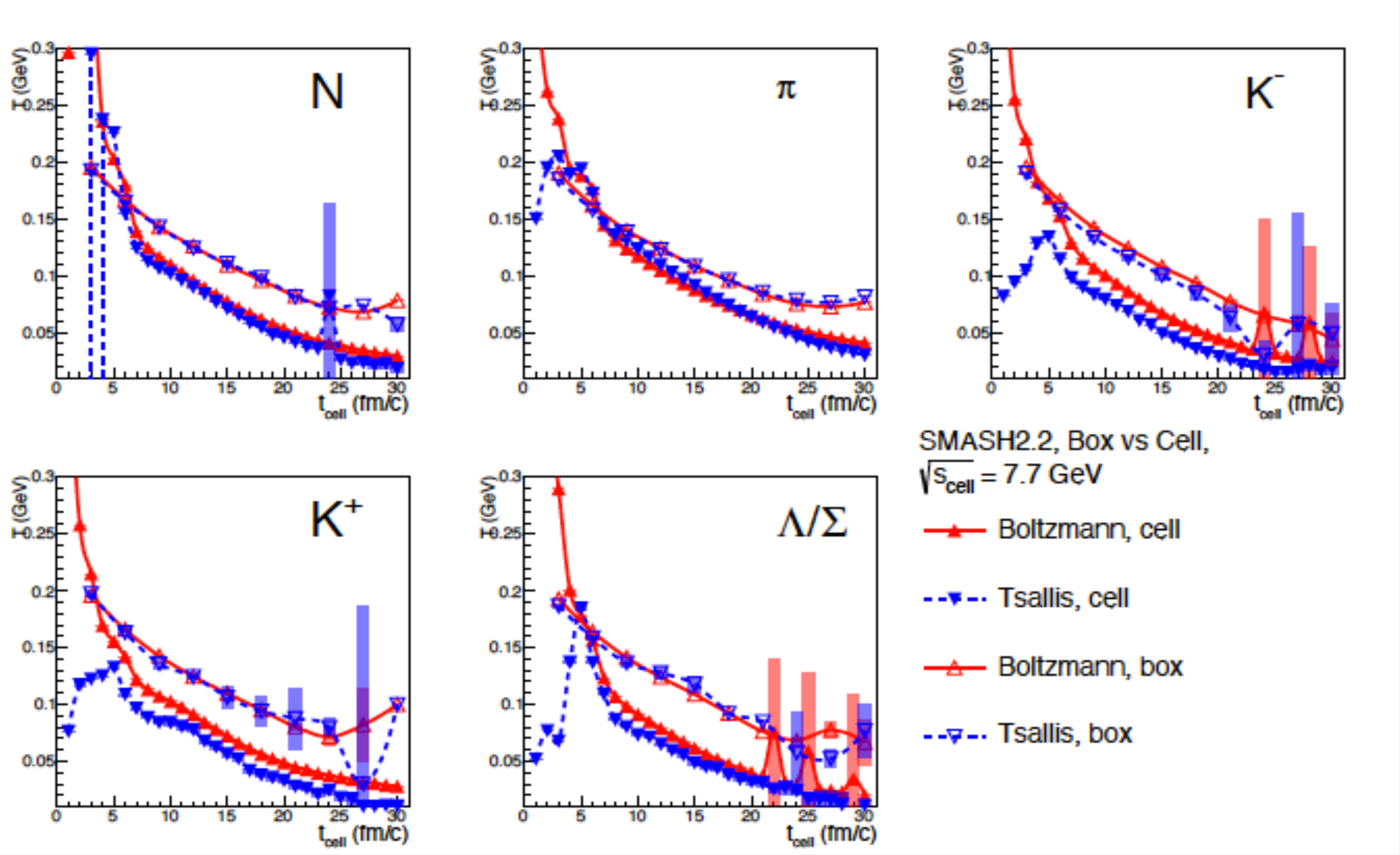

$T_{Tsallis}$ is a bit lower compered to $T_{Boltzmann}$

T IN THE CELL VS *T* IN THE BOX

Au+Au central collisions at $\sqrt{s} = 7.7$ GeV (UrQMD)

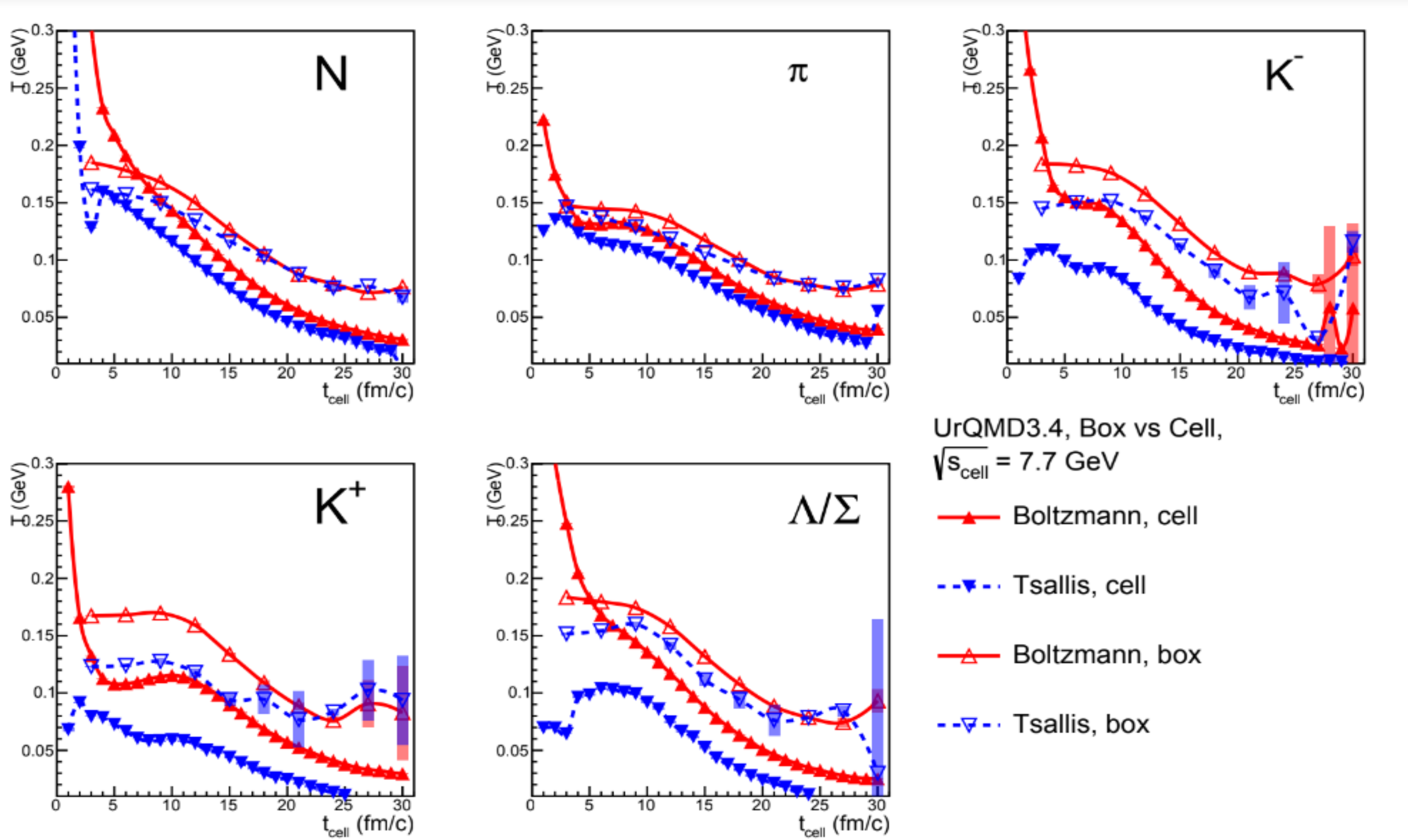

The Tsallis fit provides lower temperatures than the Boltzmann fit

CONCLUSIONS

Our study indicates that

- *Tsallis distribution better matches the particle p_T–spectra both for the matter in the cell and the infinite nuclear matter*
- ***UrQMD:*** *parameter **q** varies from **1.02** to **1.15** for the cell and from **1.01** to **1.07** for the box calculations*
- ***SMASH:*** *parameter q varies from **0.99** to **1.07** for the cell and is about $\mathbf{1 \pm 0.01}$ for the box calculations*
- q^{cell} *is close to* q^{box} *at lower energies for both models*
- *at higher energies the agreement worsens*
- *the Tsallis fit provides (a bit) lower temperatures than the Boltzmann fit*

Thank you for

your attention !

Back-up

Slides

Statistical model of ideal hadron gas

input values

output values

$$\varepsilon^{\rm mic} = \frac{1}{V}\sum_i E_i^{\rm SM}(T,\mu_{\rm B},\mu_{\rm S}),$$

$$\rho_{\rm B}^{\rm mic} = \frac{1}{V}\sum_i B_i \cdot N_i^{\rm SM}(T,\mu_{\rm B},\mu_{\rm S}),$$

$$\rho_{\rm S}^{\rm mic} = \frac{1}{V}\sum_i S_i \cdot N_i^{\rm SM}(T,\mu_{\rm B},\mu_{\rm S}).$$

Multiplicity

Energy

Pressure

Entropy density

$$N_i^{\rm SM} = \frac{V g_i}{2\pi^2\hbar^3}\int_0^\infty p^2 f(p,m_i)dp,$$

$$E_i^{\rm SM} = \frac{V g_i}{2\pi^2\hbar^3}\int_0^\infty p^2\sqrt{p^2+m_i^2}\, f(p,m_i)dp$$

$$P^{\rm SM} = \sum_i \frac{g_i}{2\pi^2\hbar^3}\int_0^\infty p^2 \frac{p^2}{3(p^2+m_i^2)^{1/2}}\, f(p,m_i)dp$$

$$s^{\rm SM} = -\sum_i \frac{g_i}{2\pi^2\hbar^3}\int_0^\infty f(p,m_i)\,[\ln f(p,m_i)-1]\,p^2 dp$$

KINETIC EQUILIBRIUM

Isotropy of velocity distributions

L.Bravina et al., PRC 60, 024904 (1999)

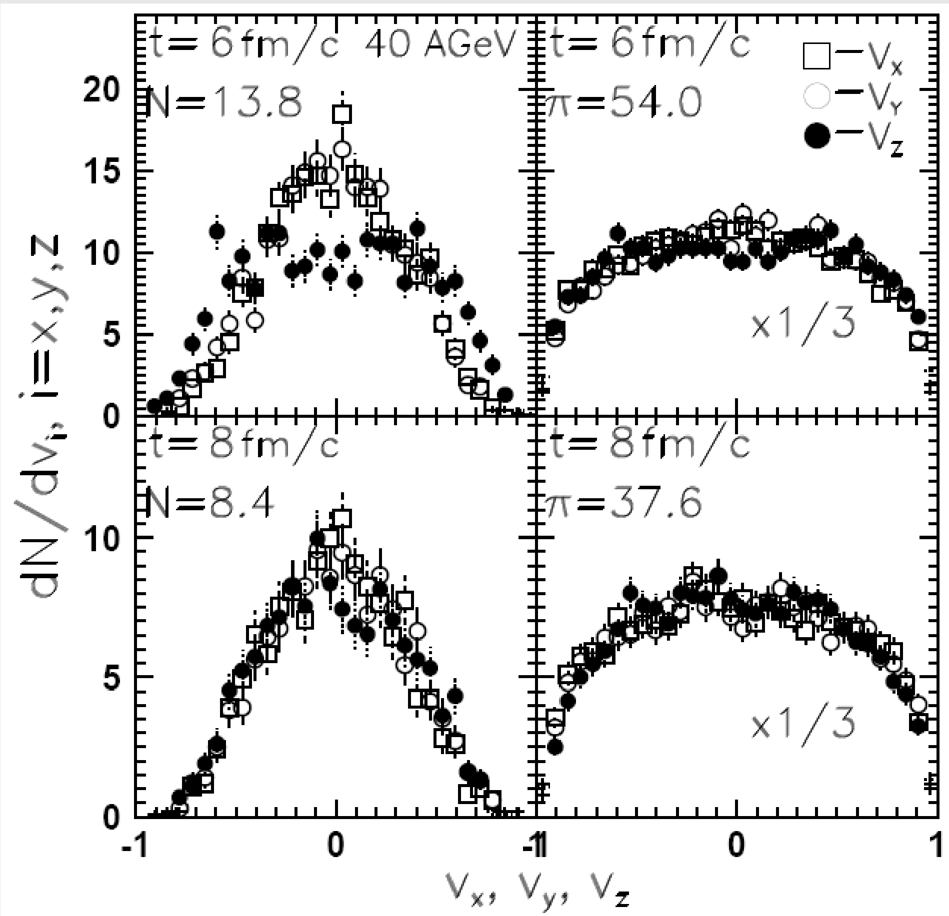

Isotropy of pressure

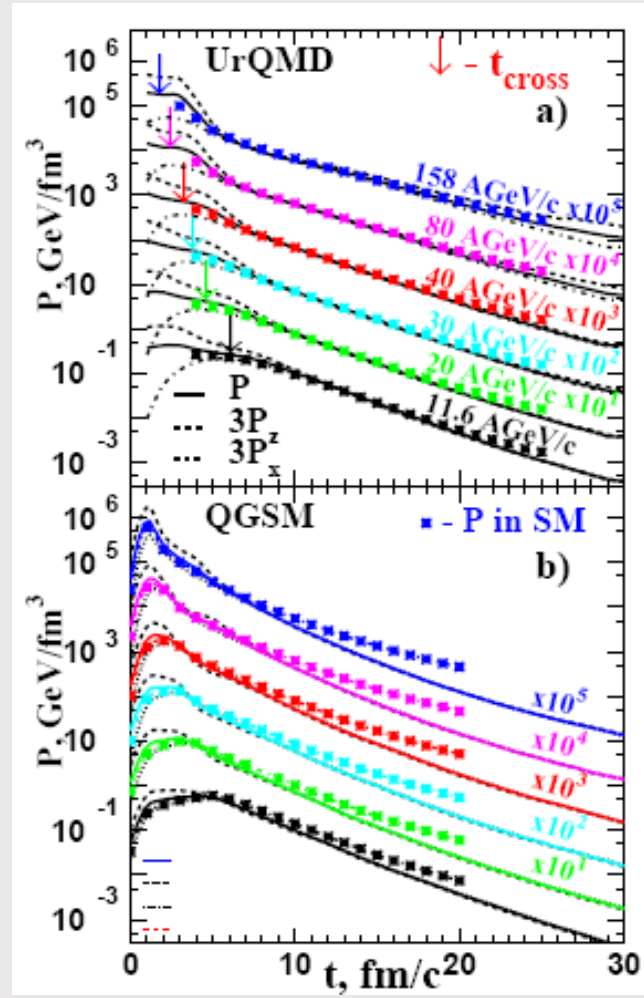

L.Bravina et al., PRC 78, 014907 (2008)

Velocity distributions and pressure become isotropic for all energies

BOX: ENERGY SPECTRA AND MOMENTUM DISTRIBUTIONS

Fit to Boltzmann distributions ~exp(-E/T)

Fit to Gaussian distributions ~ exp(- $p^2/2m_T$)

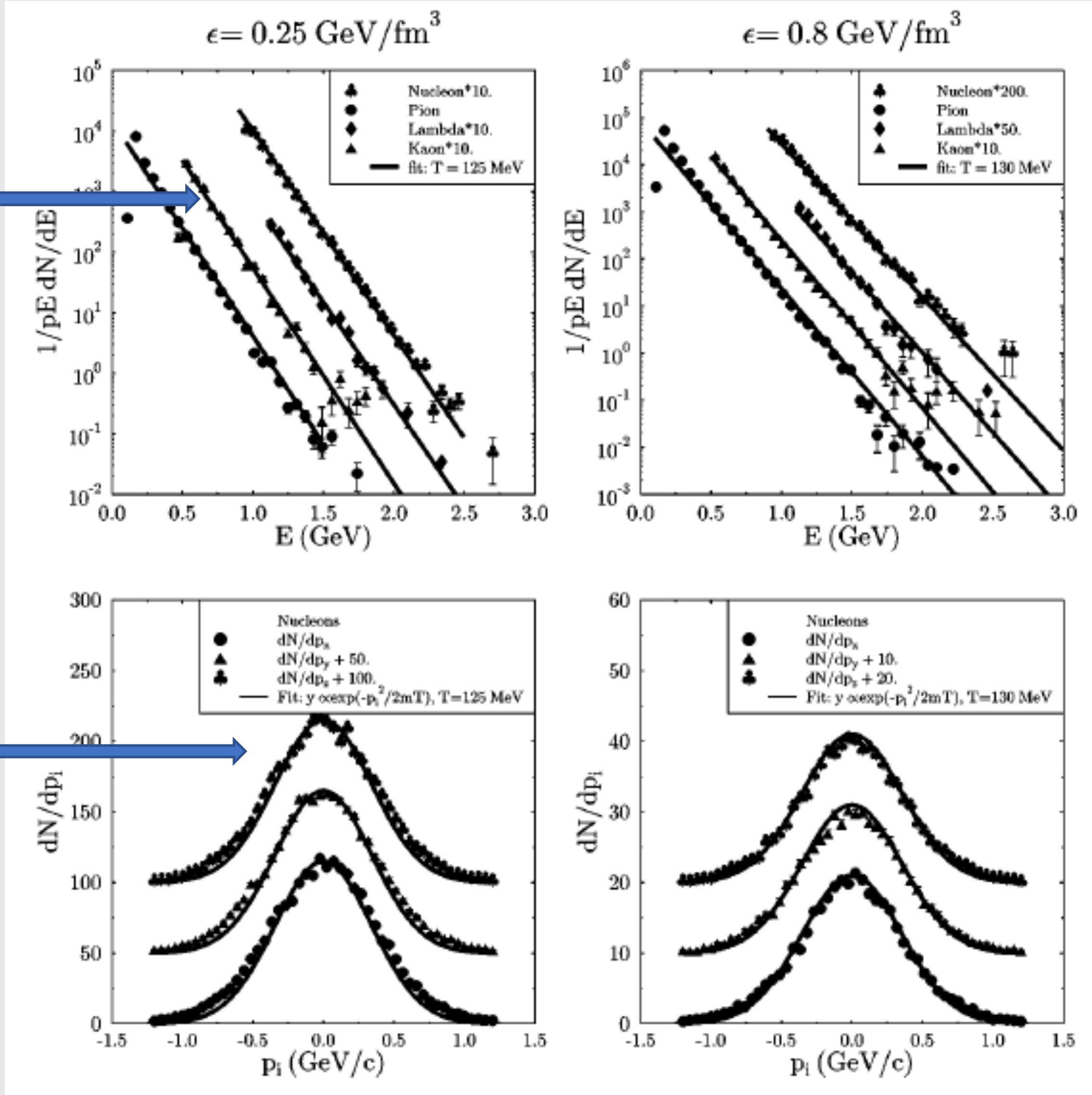

M.Belkacem et al., PRC 58, 1727 (1998)

Nearly the same temperature and complete isotropy of